ELSEVIER

Biochimica et Biophysica Acta 1467 (2000) 101–112

BIOCHIMICA ET BIOPHYSICA ACTA
BBA

www.elsevier.com/locate/bba

Partition of membrane probes in a gel/fluid two-component lipid system: a fluorescence resonance energy transfer study

Luís M.S. Loura [a,b,*], Aleksandre Fedorov [a], Manuel Prieto [a]

[a] *Centro de Química-Física Molecular, Instituto Superior Técnico, P-1049-001 Lisboa, Portugal*
[b] *Departamento de Química, Universidade de Évora, Rua Romão Ramalho, 59, P-7000-671 Évora, Portugal*

Received 10 December 1999; received in revised form 22 March 2000; accepted 31 March 2000

Abstract

A non-ideal lipid binary mixture (dilauroylphosphatidylcholine/ distearoylphosphatidylcholine), which exhibits gel/fluid phase coexistence for wide temperature and composition ranges, was studied using photophysical techniques, namely fluorescence anisotropy, lifetime and resonance energy transfer (FRET) measurements. The FRET donor, *N*-(7-nitrobenz-2-oxa-1,3-diazol-4-yl)-dilauroylphosphatidylethanolamine, and a short-tailed FRET acceptor, 1,1′-didodecil-3,3,3′,3′-tetramethylindocarbocyanine ($DiIC_{12}(3)$), were shown to prefer the fluid phase by both intrinsic anisotropy, lifetime and FRET measurements, in agreement with published reports. The other studied FRET acceptor, long-tailed probe 1,1′-dioctadecil-3,3,3′,3′-tetramethylindocarbocyanine ($DiIC_{18}(3)$), is usually reported in the literature as partitioning mainly to the gel. While intrinsic lifetime studies indeed indicated preferential partition of $DiIC_{18}(3)$ into a rigidified environment, FRET analysis pointed to an increased donor–acceptor proximity as a consequence of phase separation. These apparently conflicting results were rationalized on the basis of segregation of $DiIC_{18}(3)$ to the gel/fluid interphase. In order to fluid-located donors sense these interphase-located acceptors, fluid domains should be small (not exceed ~10–15 nm). It is concluded that membrane probes which apparently prefer the gel phase may indeed show a non-random distribution in this medium, and tend to locate in an environment which simultaneously leads to less strict packing constraints and to favorable hydrophobic matching interactions.

Keywords: Energy transfer; Gel/fluid heterogeneity; Fluorescence; Membrane domain; Membrane probe; Partition

1. Introduction

Biological membranes consist essentially of proteins and lipids. Their unique bilayer structure serves as a matrix for proteins and is made up of a wide variety of lipids [1]. The fact that they include such a large variety of lipid components, which frequently exhibit gel/gel, gel/fluid or even fluid/fluid phase separation in physiological conditions in model systems (e.g. [2]) strongly suggests the existence of lateral heterogeneity of lipid distribution (lipid domains). The detection and characterization of this kind of heter-

Abbreviations: DCM, 4-Dicyanomethylene-2-methyl-6-(*p*-dimethylaminostyryl)-4*H*-pyran; $DiIC_{12}(3)$, 1,1′-didodecil-3,3,3′,3′-tetramethylindocarbocyanine; $DiIC_{18}(3)$, 1,1′-dioctadecil-3,3,3′,3′-tetramethylindocarbocyanine; DLPC, dilauroylphosphatidylcholine; DMPC, dimyristoylphosphatidylcholine; DSPC, distearoylphosphatidylcholine; FRET, fluorescence resonance energy transfer; GUV, giant unilamellar vesicles; LUV, large unilamellar vesicles; NBD-DLPE, *N*-(7-nitrobenz-2-oxa-1,3-diazol-4-yl)-dilauroylphosphatidylethanolamine

* Corresponding author. Fax: +351-21-846-4455;
E-mail: pclloura@alfa.ist.utl.pt

0005-2736/00/$ – see front matter
PII: S0005-2736(00)00211-X

ogeneities has recently raised considerable interest in the biochemical and biophysical communities, due to the potential biological roles they may play [3]. Macrodomains (>100 nm) can be directly observed using microscopy techniques (e.g. [4,5]). However, the experimental study of microdomains (<100 nm) is more difficult, because they are smaller than the resolution limit of classic microscopy, and recent microscopic techniques with nanometer resolution are still under development [6]. In this respect, the most promising tools are probably indirect methods, such as magnetic resonance methods and photophysical techniques (e.g. [7]).

The lipid gel/fluid phase separation has been the most studied type of membrane heterogeneity, especially when it stems from differences in the length of the component's acyl chains. In the literature, conflicting values for the size of microdomains have been reported. For example, for 1:1 dimyristoylphosphatidylcholine (DMPC)/distearoylphosphatidylcholine (DSPC) mixtures, sizes ranging from 13 molecules (fluorescence quenching and Monte-Carlo simulations [8]), to 800–1500 molecules (electronic spin resonance spectroscopy [9]) or even $\sim 10^6$ molecules (fluorescence recovery after photobleaching and Monte-Carlo simulations [10]) have been published. This large range of reported domain sizes shows that even for gel/fluid domains much is still unknown.

Fluorescence resonance energy transfer (FRET; recently reviewed in [11,12]) is a non-radiative photophysical process in which a fluorescent species (the donor), initially electronically excited, transfers its excitation to another chromophore (the acceptor), the absorption of which has a spectral overlap with the donor's emission. FRET causes donor fluorescence quenching, and has a strong dependence (sixth power) on the intermolecular distance. If, instead of an isolated donor/acceptor pair at a single defined distance, there is a distribution of donor and acceptor molecules in three-dimensional space or in a plane (as expected upon incorporation of probes in membranes), donor fluorescence becomes dependent on the acceptor concentration surrounding the donors. If different donors are located in different microenvironments and are surrounded by different acceptor local concentrations, as expected in a microheterogeneous system, one can potentially extract information on the different probe concentrations in each environment from the donor fluorescence decay in presence of acceptor. Additionaly, deviations to the theoretical decay laws (derived assuming large domain sizes, typically >20 nm, and random distribution of probes) can provide unique topological information, i.e. give insight into probe aggregation (which is very relevant for the use of such molecules as fluorescent membrane probes) and detect small domains. Surprisingly, applications of FRET measurements to membranes have not taken advantage of this feature. Only recently, the random distribution of fluorescent probes in one-component fluid phospholipid vesicles was demonstrated, as well as a non-random distribution of the same probes in the gel phase, probably resulting from their segregation to defects of the gel phase structure [13]. However, to our best knowledge, quantitative time-resolved FRET studies in two-component lipid systems have not yet been published.

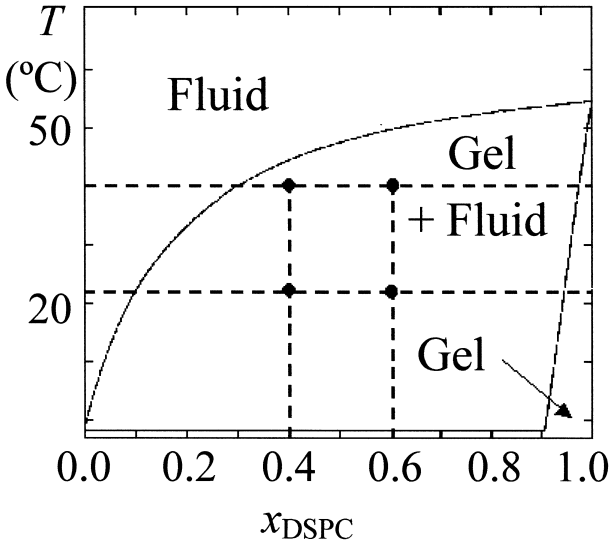

Fig. 1. Phase diagram of the DLPC/DSPC system [15]. The (T, x_{DSPC}) points studied in this work are highlighted.

As an example of a phospholipid mixture with a wide gel/fluid phase coexistence range, dilauroylphosphatidylcholine (DLPC)/DSPC was chosen. Fig. 1 shows the phase diagram for this system [14,15]. Four (temperature, DSPC mole fraction) points were studied inside the phase coexistence range: (T, x_{DSPC}) = (22°C, 0.4), (22°C, 0.6), (40°C, 0.4) and (40°C, 0.6). As fluorescent probes, lipid analogs were selected. *N*-(7-nitrobenz-2-oxa-1,3-diazol-4-yl)-dilauroylphosphatidylethanolamine (NBD-

DLPE) was used as donor, and two carbocyanine dyes with different alkyl chains, 1,1′-didodecyl-3,3,3′,3′-tetramethylindocarbocyanine ($DiIC_{12}(3)$) and 1,1′-dioctadecyl-3,3,3′,3′-tetramethylindocarbocyanine ($DiIC_{18}(3)$) were used as acceptors. From the length of the probes' chains, and only taking the hydrophobic matching effect into account [16], one expected a priori to observe donor and $DiIC_{12}(3)$ partition mostly to the fluid (DLPC rich) phase, while $DiIC_{18}(3)$ should prefer the gel (DSPC rich) phase [17,18]. This would lead to an increase in FRET efficiency for the NBD-DLPE/$DiIC_{12}(3)$ pair in the phase coexistence range relative to the values for pure phases, because both probes would be essentially located in the fluid phase, resulting in an increased local acceptor concentration. For the NBD-DLPE/$DiIC_{18}(3)$ pair, the opposite was expected, because donor and acceptor should prefer different phases, and therefore be more distant on average as a consequence of phase separation.

2. Materials and methods

2.1. Materials

The phospholipids DLPC and DSPC were purchased from Avanti Polar Lipids (Birmingham, AL) and used without further purification. The fluorescent species NBD-DLPE, $DiIC_{12}(3)$ and $DiIC_{18}(3)$ were obtained from Molecular Probes (Eugene, OR). NBD-DLPE is not available in their catalog and was purchased after custom synthesis. Its purity was verified by thin-layer chromatography in silica-gel plates (from Merck, Darmstadt, Germany), using a chloroform:methanol:water mixture (65:25:4, v/v) as elution solvent. The measured retention factor was 0.54, in agreement with the published value of 0.53 [19]. The acceptor probes were used as received.

2.2. Vesicle preparation

Adequate amounts of stock solutions of host phospholipids and probes in chloroform and methanol, respectively, were mixed, dried until complete evaporation, and suspended in buffer (Tris–HCl 50 mM, NaCl 100 mM, EDTA 0.2 mM, pH 7.4; Tris–HCl from BDH (London) and NaCl and EDTA from Merck (Darmstadt, Germany) were used). Large unilamellar vesicles (LUV) were then prepared by the extrusion method [20]. In order to ensure that the lipid mixtures were in an equilibrium state, the prepared vesicles rested overnight at 22°C, and the measurements took place on the following day.

2.3. Fluorescence measurements

Fluorescence decay measurements were carried out with a time-correlated single-photon counting system. For excitation of NBD-DLPE at 340 nm, a frequency doubled, cavity dumped dye laser of 4-dicyanomethylene-2-methyl-6-(*p*-dimethylaminostyryl)-4*H*-pyran, or DCM (Coherent 701-2), synchronously pumped by a mode-locked Ar^+ laser (514.5 nm, Coherent Innova 400-10) was used. Two filters (Corion LG-400 and LS-550) were added to a Jobin-Yvon HR320 monochromator, to respectively further screen scattered excitation light, and isolate donor fluorescence from that of acceptor. For the detection, a Hamamatsu R-2809 MCP photomultiplier was used, and the instrumental response functions (80 ps fwhm) for deconvolution were generated from a scatter dispersion (Silica, colloidal water suspension, Aldrich, Milwaukee, WI). Emission (at 520 nm) was detected at the magic angle relative to the vertically polarized excitation beam. The number of counts on the peak channel was 20 000, and the number of channels per curve used for analysis was $\sim$1000. For the experiments at 22°C, time scales of 44.1 ps/ch and 22.1 ps/ch were used in the measurement of NBD-DLPE decays in the absence and presence of acceptor, respectively. For the experiments at 40°C, the time scales were 33.8 ps/ch in the measurement of NBD-DLPE decays in the absence of acceptor and 11.0 ps/ch in the presence of acceptor. For measurement of fluorescence decays of $DiIC_{12}(3)$ and $DiIC_{18}(3)$, the same instrument was used, but excitation was now at 570 nm using Rhodamine 6G as the laser dye. Time scales were 5.53 ps/ch for measurements at 22°C and 3.83 ps/ch for measurements at 40°C. Data analysis was carried out using a non-linear, least squares iterative convolution method based on the Marquardt algorithm [21] using global analysis, i.e. in each case, different decay curves, obtained both with and without acceptor, were analyzed together, with linkage of lifetimes and pre-ex-

ponential factors ratio (for discussion on the advantages of this procedure, see [13,22]). The goodness of the fit was judged from the individual experiment's chi-square values (χ^2), global value (χ^2_G), and weighted residuals and autocorrelation plots.

Fluorescence steady-state measurements were carried out with a SLM-Aminco 8100 Series 2 spectrofluorimeter (Rochester, NY; with double excitation and emission monochromators, MC-400) in a right angle geometry. The light source was a 450 W Xe arc lamp and the reference was a Rhodamine B quantum counter solution. Correction of excitation and emission spectra was performed using the apparatus correction software. Quartz cuvettes of 5×5 mm were used. Temperature was controlled to ±0.5°C by a thermostatted cuvette holder. Both emission and excitation spectral bandwidths were 4 nm.

The steady-state anisotropy, $\langle r \rangle$, was calculated from [23]

$$\langle r \rangle = (I_{VV} - G \cdot I_{VH})/(I_{VV} + 2 \cdot G \cdot I_{VH}) \quad (1)$$

where the different intensities I_{ij} are the steady-state vertical and horizontal components of the fluorescence emission with excitation vertical (I_{VV} and I_{VH}, respectively) and horizontal (I_{HV} and I_{HH}, respectively) to the emission axis. The latter pair of components is used to calculate the G factor ($G = I_{HV}/I_{HH}$ [24]). Polarization of excitation and emission light was achieved using Glan-Thompson polarizers. Absorption spectra were carried out in a Jasco V-560 spectrophotometer. Average lifetimes, $\langle \tau \rangle$, were calculated from (e.g. [12])

$$\langle \tau \rangle = (A_1 \cdot \tau_1^2 + A_2 \cdot \tau_2^2)/(A_1 \cdot \tau_1 + A_2 \cdot \tau_2) \quad (2)$$

where τ_i are the decay lifetime components and A_i are their respective normalized amplitudes. Critical distances for energy transfer, R_0, were calculated from (e.g. [25])

$$R_0 = 0.2108 \cdot \left\{ \kappa^2 \cdot \Phi_D \cdot n^{-4} \cdot \int_0^\infty I(\lambda) \cdot \varepsilon(\lambda) \cdot \lambda^4 \cdot d\lambda \right\}^{1/6} \quad (3)$$

where Φ_D is the donor quantum yield, $\varepsilon(\lambda)$ is the acceptor molar absorption coefficient, κ^2 is the orientation factor, n is the refractive index, and λ is the wavelength. If the λ units used in Eq. 3 are nm, the calculated R_0 has Å units. The energy transfer efficiency, E, was calculated from the experimental decays of donor in the presence ($i_{DA}(t)$) and absence ($i_D(t)$) of acceptor:

$$E = 1 - \int_0^\infty i_{DA}(t) dt \Big/ \int_0^\infty i_D(t)\, dt \quad (4)$$

2.4. Quantification of probe partition from fluorescence measurements

2.4.1. Probe photophysics

The gel/fluid partition coefficient is defined by [26]

$$K_p^{g/f} = (P_G/X_G)/(P_F/X_F) \quad (5)$$

In this equation, P_G is the probe fraction in the gel phase, and X_G is the mole fraction of gel (P_F and X_F have identical meanings for the fluid phase).

Using Weber's law of additivity of anisotropy [27], one can estimate the donor gel–fluid partition coefficient. The anisotropy in a gel/fluid mixture is given by

$$\langle r \rangle = \frac{\varepsilon_G \cdot P_G \cdot \Phi_G \cdot g_G \cdot \langle r \rangle_G + \varepsilon_F \cdot P_F \cdot \Phi_F \cdot g_F \cdot \langle r \rangle_F}{\varepsilon_G \cdot P_G \cdot \Phi_G \cdot g_G + \varepsilon_F \cdot P_F \cdot \Phi_F \cdot g_F} \quad (6)$$

where ε_i is the molar absorption coefficient, Φ_i is the fluorescence quantum yield and g_i is the fluorescence intensity at the emission wavelength in a normalized spectrum, for pure i phase. Assuming $\varepsilon_F = \varepsilon_G$, $g_F = g_G$ and $\Phi_F/\Phi_G = \bar{\tau}_F/\bar{\tau}_G$ ($\bar{\tau}$ is the lifetime-weighted quantum yield, given by $\Sigma A_j \tau_j$) and using $P_G/P_F = K_p \cdot (1 - X_F)/X_F$ (from Eq. 5), the only unknown parameter is K_p, which can be determined by fitting.

The fluorescence intensity measured for a set of samples is related to the probe fraction within each phase, for dilute samples (total absorbance < 0.1), according to [28]:

$$I_F = K \cdot (P_G \cdot \varepsilon_G \cdot \Phi_G + P_F \cdot \varepsilon_F \cdot \Phi_F) \quad (7)$$

where the constant K comprises a geometric factor as well as the excitation light intensity, and the other symbols have the same meaning as in Eq. 6. This equation (together with Eq. 5) can also be used in time-resolved data analysis, if the lifetime-weighted quantum yields $\bar{\tau}$ are used instead of the fluorescence quantum yields and I_F.

2.4.2. FRET measurements

The donor fluorescence decay curve in a two-infinite-phases (gel, G, and fluid, F) system (in this way, only intraphase FRET is considered), with random distribution of donors and acceptors within each phase is given by

$$i_{DA}(t) = A_G[\exp(-t/\tau_{1G}) + q_G \cdot \exp(-t/\tau_{2G})] \cdot \rho_{cG}(t) \cdot \rho_{tG}(t) + A_F[\exp(-t/\tau_{1F}) + q_F \cdot \exp(-t/\tau_{2F})] \cdot \rho_{cF}(t) \cdot \rho_{tF}(t) \quad (8)$$

In this equation, τ_{ij} ($i = 1, 2$; $j = F, G$) are the donor decay components and q_j is the pre-exponential factor's ratio in pure phase j and in the absence of acceptors. A_j is proportional to the amount of donors in phase j. All FRET contributions to the decay are included in the $\rho_{kj}(t)$ functions ($k = c,t$; if these functions were equal to unity – which is the case for null acceptor concentration – $i_{DA}(t)$ would be the intrinsic donor decay law).

$\rho_{cj}(t)$ is the donor decay law due to FRET to acceptors in the same bilayer leaflet leaflet (*cis*) [11]:

$$\rho_{cj}(t) = \exp(-c_j t^{1/3}) \quad (9)$$

where c_j is proportional to the number of acceptors per area unit, n_j (Γ is the complete gamma function) [11]:

$$c_j = \Gamma(2/3) \cdot n_j \cdot \pi \cdot R_{0j}^2 \cdot \bar{\tau}_j^{1/3} \quad (10)$$

$\rho_{tj}(t)$, on the other hand, is the donor decay law due to FRET to acceptors in the opposite bilayer leaflet leaflet (*trans*), and is given by [29]:

$$\rho_{tj}(t) = \exp\left\{-\frac{2c_j}{\Gamma(2/3) \cdot b_j} \int_0^1 [1 - \exp(-t\, b^3\, \alpha^6)]\, \alpha^{-3} d\alpha\right\} \quad (11)$$

where $b_j = (R_{0j}/d_j)^2/\bar{\tau}_j^{1/3}$, d_j being the distance between the plane of donors in one leaflet and the plane of the acceptors in the opposite leaflet, in phase j.

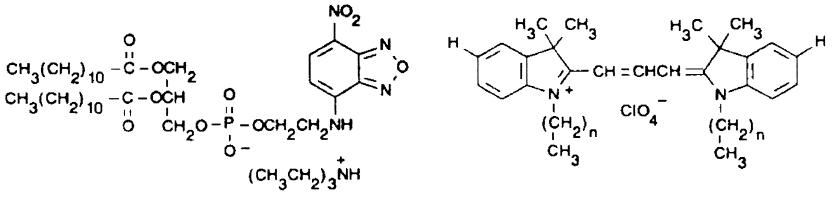

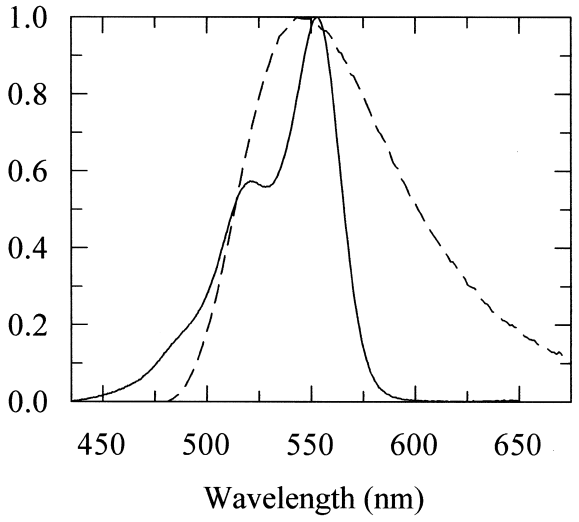

Fig. 2. Top: Structures of NBD-DLPE and DiIC$_n$(3) ($n = 11$ for DiIC$_{12}$(3), $n = 17$ for DiIC$_{18}$(3)). Bottom: corrected and normalized emission spectrum of NBD-DLPE (dashed line; $\lambda_{exc} = 467$ nm) and normalized absorption spectrum of DiIC$_n$(3) (solid line).

In the framework of Eqs. 8–11, the gel/fluid partition coefficients of donor and acceptor (K_{pD} and K_{pA}, respectively) are related to those equation's parameters according to

$$K_{pA}^{g/f} = (c_G \cdot a_G)/(c_F \cdot a_F) \quad (12)$$

$$K_{pD}^{g/f} = (A_G/X_G)/(A_F/X_F) \quad (13)$$

a_G and a_F in Eq. 12 represent the areas per lipid molecule in gel and fluid phases, respectively. In this work, they were taken as the values for DSPC at 25°C (54.7 Å^2 [2]), and DLPC at 25°C (68.7 Å^2 [2]), respectively.

3. Results

3.1. Probe photophysics and partition from anisotropy and lifetime measurements

Fig. 2 shows the structure of donor and acceptor probes, as well as the relevant spectra for FRET (donor emission and acceptor absorption). NBD-DLPE fluorescence decays in DLPC and DSPC are biexponential at both 22 and 40°C, as shown in Table 1. It is apparent that, for each temperature, both the NBD-DLPE average lifetime and anisotropy increase with the relative amount of gel phase (for all samples, NBD-DLPE:non-fluorescent lipid = 0.001, and homotransfer depolarization is negligible for this small probe concentration (result not shown)). It is particularly interesting that for $T = 22$°C the increase in both $\langle\tau\rangle$ and $\langle r\rangle$ is relatively small, the values being close to those measured in pure fluid

Table 1
Decay parameters of NBD-DLPE in LUV in the absence of acceptor[a]

Vesicle composition	$T = 22$°C	$T = 40$°C
100% DLPC	$\tau_1 = 2.17$ ns (35%) $\tau_2 = 10.3$ ns (65%) $\langle\tau\rangle = 9.51$ ns $\chi^2 = 1.33$ $X_F = 1.0$ $\langle r\rangle = 0.107$	$\tau_1 = 1.28$ ns (33%) $\tau_2 = 7.09$ ns (67%) $\langle\tau\rangle = 6.62$ ns $\chi^2 = 1.38$ $X_F = 1.0$ $\langle r\rangle = 0.066$
60% DLPC, 40% DSPC	$\tau_1 = 2.12$ ns (35%) $\tau_2 = 10.3$ ns (65%) $\langle\tau\rangle = 9.53$ ns $\chi^2 = 1.29$ $X_F = 0.63$ $\langle r\rangle = 0.110$	$\tau_1 = 1.40$ ns (34%) $\tau_2 = 7.27$ ns (66%) $\langle\tau\rangle = 6.74$ ns $\chi^2 = 1.24$ $X_F = 0.81$ $\langle r\rangle = 0.074$
40% DLPC, 60% DSPC	$\tau_1 = 2.27$ ns (35%) $\tau_2 = 10.5$ ns (65%) $\langle\tau\rangle = 9.67$ ns $\chi^2 = 1.62$ $X_F = 0.40$ $\langle r\rangle = 0.123$	$\tau_1 = 1.50$ ns (35%) $\tau_2 = 7.53$ ns (65%) $\langle\tau\rangle = 6.95$ ns $\chi^2 = 1.42$ $X_F = 0.52$ $\langle r\rangle = 0.084$
100% DSPC	$\tau_1 = 2.73$ ns (41%) $\tau_2 = 11.2$ ns (59%) $\langle\tau\rangle = 9.92$ ns $\chi^2 = 1.97$ $X_F = 0.0$ $\langle r\rangle = 0.184$	$\tau_1 = 2.45$ ns (43%) $\tau_2 = 9.22$ ns (57%) $\langle\tau\rangle = 8.08$ ns $\chi^2 = 1.90$ $X_F = 0.0$ $\langle r\rangle = 0.116$

[a]Also shown are the fluid phase fraction in each sample (X_F, from the phase diagram of Fig. 1), and the steady-state anisotropy ($\langle r\rangle$).

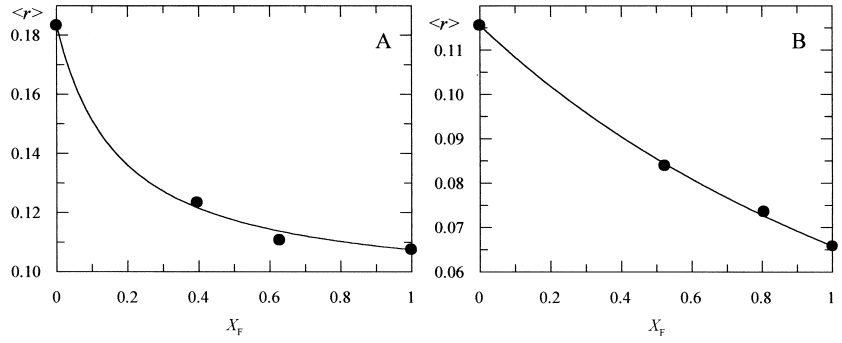

Fig. 3. NBD-DLPE anisotropy (●) versus fluid phase fraction in DLPC/DSPC LUV. The curves are fits using Eq. 6. (A) 22°C, $K_{pD} = 0.16$. (B) 40°C, $K_{pD} = 0.80$.

phase even when $x_{DSPC} = 0.6$. For $T = 40$°C, this effect is not so pronounced. The variations of $\langle\tau\rangle$ e $\langle r\rangle$ reflect the gel/fluid probe partition. From the $\langle r\rangle$ variation, and using Eqs. 5 and 6, the values $K_{pD}(22°C) = 0.16$ and $K_{pD}(40°C) = 0.80$ are obtained (see Fig. 3).

For the carbocyanine dyes, anisotropy could not be used for K_p estimation, due to the occurrence of energy migration even at low probe concentrations. The best fluorescence method for this purpose is lifetime measurement [30]. Therefore, probe lifetimes were measured for the different temperatures and compositions. Once again, the fluorescence decays are biexponential in LUV, and the $\bar{\tau}$ values increase with increasing gel phase fraction. The decay parameters for pure DLPC and DSPC vesicles are shown in Table 2. Fitting of Eqs. 5 and 7 to the $\bar{\tau}$ variation with LUV composition results in $K_p(DiIC_{12}(3), 22°C) = 0.48$ (Fig. 4A), $K_p(DiIC_{12}(3), 40°C) = 1.1$ (Fig. 4B), $K_p(DiIC_{18}(3), 22°C) = 5.2$ (Fig. 4C) and $K_p(DiIC_{18}(3), 22°C) = 2.4$ (Fig. 4D).

3.2. FRET between NBD-DLPE and $DiIC_n(3)$

As is evident from Fig. 2, there is considerable overlap between NBD-DLPE emission and $DiIC_n(3)$ absorption. Using as reference Φ(NBD-dipalmitoylphosphatidylethanolamine, room temperature) = 0.32 [31] the values Φ_D(in DLPC, 22°C) = 0.28, Φ_D(in DSPC, 22°C) = 0.29, Φ_D(in DLPC, 40°C) = 0.19, and Φ_D(in DSPC, 40°C) = 0.23 were obtained. For the maximal molar absorption coefficients of the acceptors, $\varepsilon(DiIC_{12}(3)) = 7.9 \times 10^4$ $M^{-1}cm^{-1}$ and $\varepsilon(DiIC_{12}(3)) = 8.3 \times 10^4$ $M^{-1}cm^{-1}$ were measured.

Table 2
Decay parameters of $DiIC_{12}(3)$ and $DiIC_{18}(3)$ in pure DLPC and DSPC vesicles at 22 and 40°C

Probe, LUV composition	$T = 22$°C	$T = 40$°C
$DiIC_{12}(3)$, DLPC	$\tau_1 = 0.56$ ns (80%) $\tau_2 = 1.44$ ns (20%) $\chi^2 = 1.71$	$\tau_1 = 0.30$ ns (83%) $\tau_2 = 1.00$ ns (17%) $\chi^2 = 1.49$
$DiIC_{12}(3)$, DSPC	$\tau_1 = 0.63$ ns (51%) $\tau_2 = 1.51$ ns (49%) $\chi^2 = 1.14$	$\tau_1 = 0.38$ ns (52%) $\tau_2 = 0.91$ ns (48%) $\chi^2 = 1.08$
$DiIC_{18}(3)$, DLPC	$\tau_1 = 0.56$ ns (77%) $\tau_2 = 1.34$ ns (23%) $\chi^2 = 1.33$	$\tau_1 = 0.31$ ns (74%) $\tau_2 = 0.74$ ns (26%) $\chi^2 = 1.22$
$DiIC_{18}(3)$, DSPC	$\tau_1 = 0.69$ ns (32%) $\tau_2 = 1.73$ ns (68%) $\chi^2 = 1.07$	$\tau_1 = 0.46$ ns (40%) $\tau_2 = 1.16$ ns (60%) $\chi^2 = 1.04$

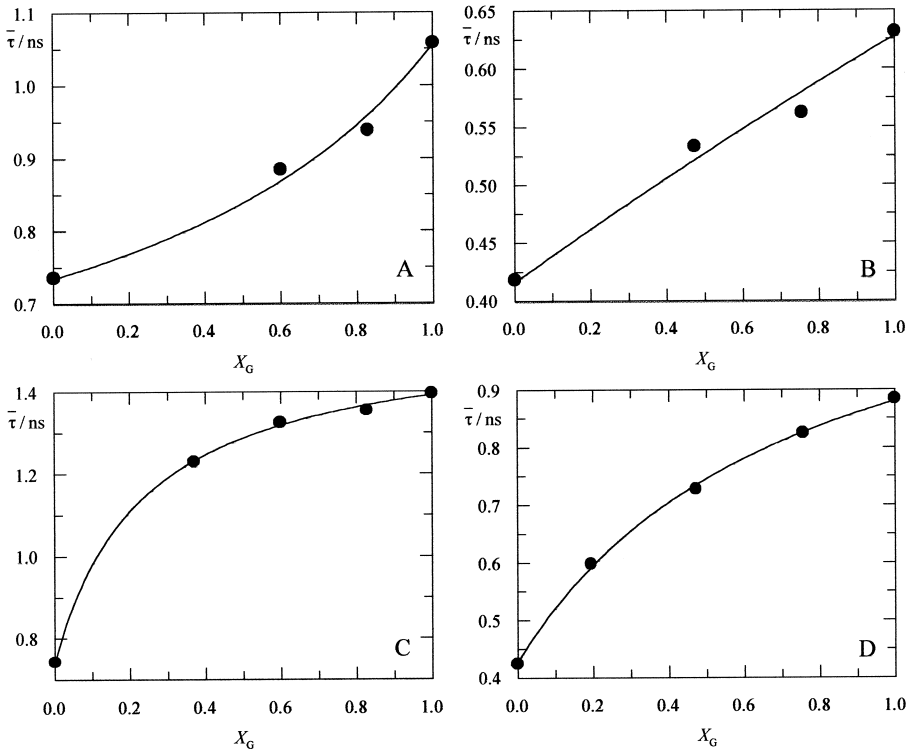

Fig. 4. $DiIC_{12}(3)$ (A,B) and $DiIC_{18}(3)$ (C,D) lifetime-weighted quantum yields in DLPC/DSPC LUV versus gel phase fraction (X_G), at 22°C (A,C) and 40°C (B,D). Probe concentration was 0.03 mol%. The curves are fits using Eq. 7 to the experimental data (with K_p = 0.48 in A, 1.1 in B, 5.2 in C and 2.4 in D).

These values, together with $\kappa^2 = 2/3$ (isotropic dynamic limit; note that even if the transfer regime is not strictly isotropic or dynamic, as may be expected, the presented FRET analysis is still valid, as discussed in detail in [13]) and $n = 1.4$ [29] result in $R_0 = 5.2$ nm (22°C, both in DLPC and in DSPC), $R_0 = 4.9$ nm (40°C, DLPC) and $R_0 = 5.0$ nm (40°C, DSPC).

The cosolubilization procedure in the preparation of LUV leads to a distribution, presumably symmetric, of probes on both bilayer leaflets. In this situation, time-resolved FRET results were analyzed using Eqs. 8–11. d_G in Eq. 11 was approximated to the value for DSPC (45.5 Å for $T = 25$°C [2]), while d_F was taken as that of DLPC (30.0 Å for $T = 25$°C [2]). This is an acceptable approximation, given the non-ideality of the system: the gel phase is much richer in DLPC, and the opposite is true for the fluid phase. Therefore, we have $b_G = 0.61$ $ns^{-1/3}$ and $b_F = 1.41$ $ns^{-1/3}$.

The fluorescence decays of NBD-DLPE were measured at both $T = 22$°C and 40°C, for $x_{DSPC} = 0.40$ and 0.60, and in absence and presence

Table 3
Results of global analysis of the fluorescence decays of NBD-DLPE in presence and absence of either $DiIC_{12}(3)$ or $DiIC_{18}(3)$, in DLPC/DSPC LUV

	$T = 22$°C	$T = 40$°C
100% DLPC, 0% DSPC		
τ_{1F}/ns (pre-exponential)	2.0 (34%)	1.2 (33%)
τ_{2F}/ns (pre-exponential)	10.3 (66%)	7.1 (67%)
60% DLPC, 40% DSPC		
K_{pD}	0.21	0.53
K_{pA} ($DiIC_{12}(3)$)	0.11	0.12
K_{pA} ($DiIC_{18}(3)$)	0.15	0.05
40% DLPC, 60% DSPC		
K_{pD}	0.41	0.41
K_{pA} ($DiIC_{12}(3)$)	0.14	0.12
K_{pA} ($DiIC_{18}(3)$)	0.15	0.07
100% DLPC, 0% DSPC		
τ_{1F}/ns (pre-exponential)	2.8 (41%)	2.6 (44%)
τ_{2F}/ns (pre-exponential)	11.2 (59%)	9.3 (56%)
Global χ^2	1.39	1.33

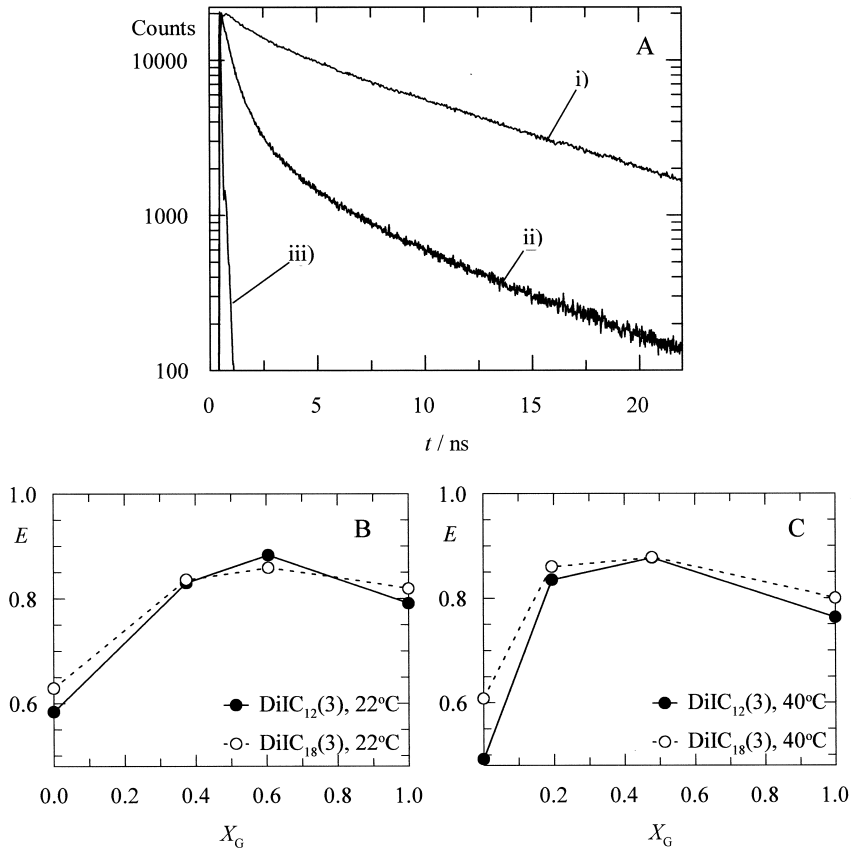

Fig. 5. (A) i, Fluorescence decay of NBD-DLPE (0.1 mol%) in DLPC/DSPC LUV ($x_{DSPC} = 0.4$); ii, Same as i, but in the presence of $DiIC_{12}(3)$ (1.4 mol%); iii, laser excitation profile. (B,C): FRET efficiency versus gel phase fraction. The ratios $DiIC_{12}(3)$:total lipid and $DiIC_{18}(3)$:total lipid are 0.014 and 0.018, respectively.

of either acceptor. Fig. 5A shows typical decay curves of donor fluorescence in absence and presence of acceptor, for a given composition and temperature. Prior to analysis of the experimental decay curves with the above formalism, one can gain information from the variation of E along a tie-line of the phase diagram. This is shown in Fig. 5B for $DiIC_{12}(3)$:total lipid = 0.014 and $DiIC_{18}(3)$:total lipid = 0.018. As in the gel phase, the area a per lipid molecule is smaller than in the fluid phase, the acceptor concentration is larger, and it is therefore expected that $E(X_G = 1.0) > E(X_G = 0.0)$ (note that R_0 is virtually identical in both phases). This is indeed observed for both probes at both temperatures. The variation of E inside the gel/fluid coexistence range ($0.0 < X_G < 1.0$) is dictated by the relative affinities of the probes for the different phases, as discussed at the end of Section 1.

Fig. 5B shows that, for both acceptors and for both temperatures, E is actually larger in the studied points in the phase coexistence range than in either pure phase. This indicates that both acceptors prefer to be located in the same phase as the donor. This phase, as shown by the variation of $\langle r \rangle$(NBD-DLPE) with the LUV composition (Fig. 3), is the fluid. While this is the behavior expected for $DiIC_{12}(3)$, the result for $DiIC_{18}(3)$ is very surprising.

In Table 3, the results of global analysis of the FRET decays are shown. For each temperature, all decays obtained at the same temperature were globally analyzed, and the parameters which are common to all samples, the donor gel lifetimes τ_{1G} and τ_{2G}, the donor pre-exponential ratio for the pure gel phase q_G, and the equivalent parameters for the fluid, τ_{1F}, τ_{2F} e q_F (see Eq. 8), are linked through the whole set of experiments.

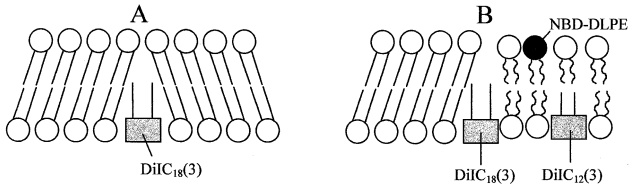

Fig. 6. (A) Schematic representation of the proposed distribution for $DiIC_{18}(3)$ in gel phase. The probe is located mainly in the gel phase defects. (B) Schematic representation of the proposed distributions for NBD-DLPE, $DiIC_{12}(3)$ and $DiIC_{18}(3)$ in a gel/fluid mixture. The 'gel-phase' probe is located mainly in the gel/fluid interphase.

4. Discussion

In this work, a gel/fluid phase-separated lipid mixture was studied using fluorescence techniques, namely fluorescence anisotropy, lifetimes and FRET, using the probes NBD-DLPE, $DiIC_{12}(3)$ and $DiIC_{18}(3)$. These probes have been used commonly by other authors in the past, and, in particular, their gel/fluid partition behavior has been investigated. NBD-DLPE is often used in fluorescence recovery after photobleaching studies, in which, precisely from the variation of $\langle r \rangle$ with X_F, it is usually assumed that it partitionates exclusively to the fluid phase in DMPC/DSPC mixtures (e.g. [10,17]). Both the anisotropy results and those from the global analysis of decays of samples with and without acceptor confirm this behavior.

Regarding the carbocyanine probes, while the results for $DiIC_{12}(3)$ (see Fig. 4A,B and Table 3) generally agree with those reported in the literature (e.g. $K_p = 0.17$ for the partition between a fluid phase, rich in a spin probe, and a DSPC-rich gel phase at $T = 21°C$ [18]), the picture is less clear for $DiIC_{18}(3)$. This probe has been reported to partition preferably to the gel phase ($K_p = 11$ at 21°C and 2.5 at 35°C in the system referred above [18]), as expected. This behavior is clearly observed in the $DiIC_{18}(3)$ lifetime measurements, as shown in Fig. 4C,D. The K_p decrease upon increasing temperature observed for $DiIC_{18}(3)$, and the opposite behavior for $DiIC_{12}(3)$, also agrees with published results [32]. The transition enthalpy of $DiIC_{18}(3)$ from the fluid to the gel is negative, and the opposite holds for $DiIC_{12}(3)$, hence the observed behavior (according to Van't Hoff's law).

However, the FRET analysis results for $DiIC_{18}(3)$ are totally at variance with the scenario described above. We verified that even for pure gel phase, it is necessary to consider two c parameters in Eqs. 8–11 for the analysis of FRET decays to this probe (result not shown). This means that $DiIC_{18}(3)$ is not randomly distributed in the gel phase, contrary to the hypothesis in Eqs. 8–11. Non-randomness of distribution of a carbocyanine probe in pure gel phase was observed in a previous work [13]. The FRET results were then explained assuming segregation of a significant amount of acceptor molecules to grain boundaries which separate ordered gel domains (Fig. 6A). It seems very plausible that a similar effect occurs in a gel/fluid mixture: a significant amount of $DiIC_{18}(3)$ molecules, higher than those dispersed in the ordered gel phase, is segregated to its domain boundaries, which, in this system, correspond to the gel/fluid interphase. This situation is schematically depicted in Fig. 6B.

The effect of this segregation upon FRET efficiency is certainly highly dependent on the domain size. For a DMPC/DSPC mixture with $X_F = 0.5$, Sankaram et al. [9] estimated the fluid domain size as 400 molecules. Considering a circular shape, this would mean domains with radius ~ 9 nm. The average distance between a donor inside such a domain and the gel/fluid interphase would be $\sim 9/3 = 3$ nm, less than R_0 in this system. This suggests that most donors in the fluid phase are indeed sensitive to the acceptors segregated in the gel/fluid interphase. If most acceptors are located in this interphase, and only a minority are dispersed inside the gel, it is not surprising that phase separation leads to an increase in FRET efficiency. In any case, FRET efficiency would still be somewhat lower than that observed for $DiIC_{12}(3)$, which is expected to be distributed inside the fluid phase, together with the donor molecules. This is indeed verified, as shown in Fig. 5B. It is also understandable that $K_{pA}(DiIC_{18}(3))$ recovered from FRET analysis is much less than unity, because most of the acceptors associated to the gel phase are, in fact, segregated in the interphase, while those associated to the fluid would be dispersed inside this phase (and their number would be artificially enlarged due to those in the interphase, which would also be sensed by the donors located inside the fluid). The FRET results for $DiIC_{18}(3)$ thus indicate two phenomena: the ocur-

rence of small (not greater than ca. 2–3 R_0, or 10–15 nm) fluid domains (otherwise, donors in the fluid would not sense the interphase in the FRET experiment) and the preference of $DiIC_{18}(3)$ for the gel/fluid interphase. These two effects are not independent, because the accumulation of solutes in the interphase region leads to a reduction in interphase tension, eventually stabilizing small domains. In a recent fluorescence microscopy study of DLPC/dipalmitoylphosphatidylcholine giant unilamellar vesicles (GUV) [5], the fluorescence of the gel phase probe ($DiIC_{20}(3)$) was spatially located in a linear, ramified topology, in general agreement with our results. The differences in domain sizes are probably due to the much larger size of GUV, as compared to LUV.

In this situation, how can one explain the $K_{pA}(DiIC_{18}(3))$ recovered from lifetime measurements? One should take into account that these measurements, contrary to the FRET decays, do not reflect distances and sizes, but only the immediate vicinity of probes. The fluorescence lifetime of $DiIC_{18}(3)$, be it in the border between gel and fluid domains, be it on grain boundaries between pure gel domains, should still be considerably higher than the value observed in pure fluid phase, which originates the variation depicted in Fig. 4C,D. In other words, a $DiIC_{18}(3)$ molecule, even if it is not fully 'immersed' in the gel, but located in a region between the gel and fluid phases, should already have its non-radiative de-excitation processes rather limited, so that its measured lifetime is considerably larger than in pure fluid phase.

The present study reveals that even a probe widely regarded in the literature as preferring markedly the gel phase may be distributed non-randomly in this ordered medium, and accumulate in the gel/fluid interphase. There is a competition between two opposite effects: on the one hand, the hydrophobic matching effect (acyl chain matching [16]) would lead these acceptor molecules to be located inside the gel phase and avoid the fluid; on the other hand, the phospholipid packing being much stricter and more compact in the gel phase than in the fluid phase, it should be much easier to incorporate a probe molecule (especially if it is not a true phospholipid) in the latter phase. The preferential location of $DiIC_{18}(3)$ in the interphase, compatible with all results described, is a compromise between these two factors. This system exemplifies a FRET application in the study of the distribution of membrane probes, which, if complemented with additional independent measurements (in this case, lifetimes), allows knowledge of detailed topological information, which is not available to most other techniques.

It is relevant to ask if there are 'well-behaved' gel phase probes. While it is impossible to generalize from this case, these studies indicate that a probe which eventually distributes randomly in the gel must have a structure virtually identical to that of the phospholipid predominant in this phase, with very minor differences, both in the headgroups and in the tails. Otherwise, the probe packing inside the gel will be difficult, probably resulting in segregation into gel defects (if there is no other coexisting phase) or into the gel/fluid interphase (in the case of gel/fluid phase coexistence). For fluid/fluid heterogeneities, which are traditionally most difficult to characterize, e.g. those obtained for phosphatidylcholine/cholesterol mixtures (e.g. [33]), these problems should not be so critical, as long as moderate probe concentrations are used. Studies using FRET in this kind of system are currently underway.

Acknowledgements

This work was supported by PRAXIS XXI (M.C.T., Portugal), project PRAXIS/P/SAU/14025/1998. L.M.S.L. acknowledges a grant (BD 3927/94) from PRAXIS XXI (Portugal). A.F. acknowledges M.C.T. for financial support.

References

[1] R.B. Gennis, Biomembranes, Springer, New York, NY, 1993.
[2] D. Marsh, CRC Handbook of Lipid Bilayers, CRC Press, Boca Raton, FL, 1990.
[3] O.G. Mouritsen, O.S. Anderson (Eds.), Topical issue: in search of a new biomembrane model. Biol. Skr. Dan. Vid. Selsk. 49 (1998) 1–214.
[4] M. Glaser, Comments Mol. Cell Biophys. 8 (1992) 37–51.
[5] J. Korlach, P. Schwille, W.W. Webb, G.W. Feigenson, Proc. Natl. Acad. Sci. USA 96 (1999) 8461–8466.
[6] C. Gliss, H. Clausen-Schaumann, R. Günter, S. Odenbach, O. Randl, T.M. Bayerl, Biophys. J. 74 (1998) 2443–2450.

[7] J. Lehtonen, P.K.J. Kinnunen, Biophys. J. 72 (1997) 1247–1257.
[8] B. Piknová, D. Marsh, T.E. Thompson, Biophys. J. 71 (1996) 892–897.
[9] M.B. Sankaram, D. Marsh, T.E. Thompson, Biophys. J. 63 (1992) 340–349.
[10] F.P. Coelho, W.L.C. Vaz, E. Melo, Biophys. J. 72 (1997) 1501–1511.
[11] B. Van Der Meer, G. Coker, III, S.-Y.S. Chen, Resonance Energy Transfer: Theory and Data, VCH Publishers, New York, NY, 1994.
[12] J.R. Lakowicz, Principles of fluorescence spectroscopy, 2nd edn., Kluwer Academic/Plenum Publishers, New York, NY, 1999.
[13] L.M.S. Loura, A. Fedorov, M. Prieto, Biophys. J. 71 (1996) 1823–1836.
[14] S. Mabrey, J.M. Sturtevant, Proc. Natl. Acad. Sci. USA 73 (1976) 3862–3866.
[15] F. Dumas, M.M. Sperotto, M.C. Lebrun, J.F. Tocanne, O.G. Mouritsen, Biophys. J. 73 (1997) 1940–1953.
[16] O.G. Mouritsen, M. Bloom, Biophys. J. 46 (1984) 141–153.
[17] W.L.C. Vaz, E.C.C. Melo, T.E. Thompson, Biophys. J. 56 (1989) 869–876.
[18] C.H. Spink, M.D. Yeager, G.W. Feigenson, Biochim. Biophys. Acta 1023 (1990) 25–33.
[19] T. Arvinte, K. Hildenbrand, Biochim. Biophys. Acta 775 (1984) 86–94.
[20] M.R. Hope, M.B. Bally, G. Webb, P.R. Cullis, Biochim. Biophys. Acta 812 (1985) 55–65.
[21] D.W. Marquardt, J. Soc. Ind. Appl. Math. (SIAM J.) 11 (1963) 431–441.
[22] J.M. Beechem, E. Gratton, M. Ameloot, J.R. Knutson, L. Brand, in: J.R. Lakowicz (Ed.), Topics in Fluorescence Spectroscopy, Vol. 2, Principles, Plenum Press, New York, NY, 1991, pp. 241–305.
[23] A. Jablonski, Bull. Acad. Pol. Sci. Ser. A 8 (1960) 259–264.
[24] R. Chen, R.L. Bowman, Science 147 (1965) 729–732.
[25] M.N. Berberan-Santos, M.J.E. Prieto, J. Chem. Soc. Faraday Trans. 283 (1987) 1391–1409.
[26] L. Davenport, Methods Enzymol. 278 (1997) 487–512.
[27] G. Weber, Biochem. J. 51 (1952) 145–155.
[28] M. Ameloot, N. Boens, R. Andriessen, V. Van der Bergh, F.C. De Schryver, J. Phys. Chem. 95 (1991) 2041–2047.
[29] L. Davenport, R.E. Dale, R.H. Bisby, R.B. Cundall, Biochemistry 24 (1985) 4097–4108.
[30] B.S. Packard, D.E. Wolf, Biochemistry 24 (1985) 5176–5181.
[31] A. Chattopadhyay, Chem. Phys. Lipids 53 (1990) 1–15.
[32] C.H. Spink, D. Clouser, J. O'Neil, Biochim. Biophys. Acta 1191 (1994) 164–172.
[33] M.R. Vist, J.H. Davis, Biochemistry 29 (1990) 451–464.